

Geophysical Research Letters

RESEARCH LETTER

10.1029/2020GL088684

Key Points:

- We assess co-occurrence and covariation between precipitation extremes and floods to explore the range of their relationships
- The spatial pattern of changes in precipitation extremes explains less than 20% of the spatial pattern of changes in floods
- Most catchments have a covariation of less than 0.5 between annual precipitation extremes and annual floods

Supporting Information:

- Supporting Information S1

Correspondence to:

H. X. Do,
hongdo@umich.edu

Citation:

Do, H. X., Mei, Y., & Gronewold, A. D. (2020). To what extent are changes in flood magnitude related to changes in precipitation extremes? *Geophysical Research Letters*, 47, e2020GL088684. <https://doi.org/10.1029/2020GL088684>

Received 1 MAY 2020

Accepted 8 SEP 2020

Accepted article online 14 SEP 2020

To What Extent Are Changes in Flood Magnitude Related to Changes in Precipitation Extremes?

Hong Xuan Do^{1,2} , Yiwen Mei¹ , and Andrew D. Gronewold¹ 

¹School for Environment and Sustainability, University of Michigan, Ann Arbor, MI, USA, ²Faculty of Environment and Natural Resources, Nong Lam University, Ho Chi Minh City, Vietnam

Abstract Despite increasing evidence of intensification of extreme precipitation events associated with a warming climate, the magnitude of peak river flows is decreasing in many parts of the world. To better understand the range of relationships between precipitation extremes and floods, we analyzed annual precipitation extremes and flood events over the contiguous United States from 1980 to 2014. A low correlation (less than 0.2) between changes in precipitation extremes and changes in floods was found, attributable to a small fraction of co-occurrence. The covariation between precipitation extremes and floods is also substantially low, with a majority of catchments having a coefficient of determination of less than 0.5, even among the catchments with a relatively high fraction of annual maxima precipitation that can be linked to floods. The findings indicate a need for more investigations into causal mechanisms driving a nonlinear response of floods to intensified precipitation extremes in a warming climate.

1. Introduction

Among the most important implications of global climate change is the intensification of the hydrologic cycle (Huntington, 2006), including the intensification of rainfall extremes (Westra et al., 2014). As air temperature rises, the water vapor held in the atmosphere also increases following the Clausius-Clapeyron relation (Clausius, 1850). This relationship has been documented extensively in the climate literature (Donat et al., 2013; Guerreiro et al., 2018; Papalexiou & Montanari, 2019; Westra et al., 2013) and has led to concerns of a future characterized broadly by an increase in the magnitude of global flood events.

Large-scale investigations into changes in floods, however, indicate a broad range of global flood response, with many studies documenting sites with a decrease in flood magnitude (Do et al., 2017; Do, Zhao, et al., 2020; Gudmundsson et al., 2019; Hodgkins et al., 2017; Kundzewicz et al., 2004; Lins & Slack, 1999). These somewhat unexpected relationships between trends in extreme precipitation and trends in extreme discharge can be attributed to the influence of other flood generation mechanisms such as soil moisture (Ivancic & Shaw, 2015; Wasko et al., 2020; Ye et al., 2017) and snow dynamics (Berghuijs et al., 2016; Blöschl et al., 2017; Do, Westra, et al., 2020; Ledingham et al., 2019; Stein et al., 2020). Even when floods are triggered by precipitation extremes, the relationship between precipitation magnitude and flood magnitude is likely nonlinear (Sharma et al., 2018), owing to the complex interactions of many variables which have undergone substantial changes such as land cover (Archfield et al., 2016; Keenan et al., 2015; Lambin et al., 2003), river channels (Slater et al., 2015; Yamazaki et al., 2014), and evapotranspiration (Bosilovich et al., 2005; Gronewold & Stow, 2014).

However, there is still limited quantitative understanding of the relationship between precipitation extremes and floods (Ivancic & Shaw, 2015; Sharma et al., 2018). A lack of discharge observations in many parts of the world (Do et al., 2018; Do, Zhao, et al., 2020) is arguably one of the main reasons for the limited evidence for how flooding responses to intensifying precipitation extremes. Even for regions with relatively good stream-flow records, empirical investigations have primarily focused on the consistency between the timing of precipitation extremes and that of floods (Berghuijs et al., 2019; Blöschl et al., 2017; Do, Westra, et al., 2020; Ivancic & Shaw, 2015; Stein et al., 2020; Wasko et al., 2020) rather than covariation between precipitation extreme intensity and flood magnitude. As a result, it is difficult to identify generalized relationships between changes in precipitation extremes and changes in floods, which is essential to the design of robust flood prevention and mitigation strategies in a warming climate (Milly et al., 2008).

We aim to fill this gap through an empirical assessment of the covariation of precipitation extremes and flood magnitude using a large sample (671) of catchments across the contiguous United States (CONUS)

(section 2.1). We used annual maxima streamflow from 1980 to 2014 from these catchments as the flood population, and we used three metrics of annual maxima precipitation to represent precipitation extremes (section 2.2). Temporal changes in floods and precipitation extremes were then estimated at each catchment, and the correlation between the spatial patterns of these trends was assessed (section 2.3). The ordinal date of precipitation extreme events was then compared to that of annual flood events (section 2.4) to assess potential linkages between these hydroclimatic extremes. Finally, the covariation between the intensity of precipitation extremes and flood magnitude across catchments was assessed (section 2.5) to evaluate the appropriateness of using changes in extreme precipitation as a proxy for changes in floods.

2. Data and Methods

2.1. Data

Data for our analysis were derived from the Catchment Attributes and Meteorology for Large-sample Studies (CAMELS) data set (Addor et al., 2017b; Newman et al., 2015). The CAMELS database aggregates a variety of hydrometeorological variables (primarily derived from other studies) for 671 catchments across the CONUS (the outlets of CAMELS catchments are shown in Figure 1). The catchments in the CAMELS database are intended to reflect relatively natural hydrologic conditions (the impervious surface area of each catchment is less than 5% of the total catchment area; see Newman et al., 2015 for more information). These catchments have a relatively small size (the median catchment area is 340.7 km²) and cover a range of climatic conditions (e.g., dry, temperate, and continental climates) as well as geographic features (e.g., mountains and deserts). Other variables in the CAMELS database include daily streamflow (originally obtained from the U.S. Geological Survey), catchment-average daily precipitation and temperature (derived from the Daymet data set; Thornton et al., 1997), and daily evapotranspiration, simulated by the conceptual SAC-SMA model (Burnash et al., 1973).

In addition to the hydrometeorological data available through CAMELS, we also obtained soil moisture data from the NOAA Climate Prediction Center (Van den Dool et al., 2003). This data set provides monthly soil moisture water height equivalent, simulated by a leaky bucket model, with a 0.5° longitude-latitude resolution. We used monthly soil moisture from the cell containing each catchment outlet as a proxy for catchment wide to obtain soil moisture conditions from 1980 to 2014. We believe this approach is appropriate for the CAMELS catchments, given their relatively small size.

2.2. Identifying Streamflow and Precipitation Extremes

Our approach to quantifying rainfall and streamflow extremes is based on the annual maxima (AMAX) index, one of the most common indices for assessing temporal changes in hydroclimatic extremes (Do et al., 2017; Kundzewicz et al., 2004; Ledingham et al., 2019; Villarini & Smith, 2010; Westra et al., 2013). We first processed streamflow data to obtain the magnitude (Q_{MAX} index; MAX denotes the magnitude of annual maxima) and the timing (Q_{DOYMAX} index; DOYMAX denotes the ordinal date of annual maxima) for each AMAX streamflow event. To reduce the chance of misattributing flood events, we omitted any years missing more than 15% of daily values. We note that more than 95% of all data years have a complete observation set, and thus, this missing data criterion has a minor influence on the analyses.

We then processed daily precipitation to derive three sets of variables, each representing a different approach to quantifying precipitation extremes. The first variable is AMAX precipitation (P), which is defined using the same approach to that of AMAX streamflow. The second precipitation variable is AMAX precipitation based only on months in which soil moisture was above average. This second variable allows us to assess the impact of constraining the timing of precipitation extremes to seasons when the catchments are wet and when floods are more likely to occur (Ivancic & Shaw, 2015). The third precipitation variable is AMAX of *effective* precipitation (Berghuijs et al., 2016, 2019), which takes into account catchment saturation and snow dynamics. We calculated this variable using a coupled soil-snow routine (Berghuijs et al., 2016; Hock, 2003; Stein et al., 2020; Woods, 2009) based on daily precipitation, temperature, and evapotranspiration (all readily available in the CAMELS data set). Details of this routine are provided in the supporting information; for further reading, see Stein et al. (2020).

Finally, we calculated the intensity and timing of each of the three precipitation AMAX variables, leading to a total of six precipitation indices: P_{MAX} and P_{DOYMAX} (for the first precipitation variable), $P_{sm,MAX}$ and

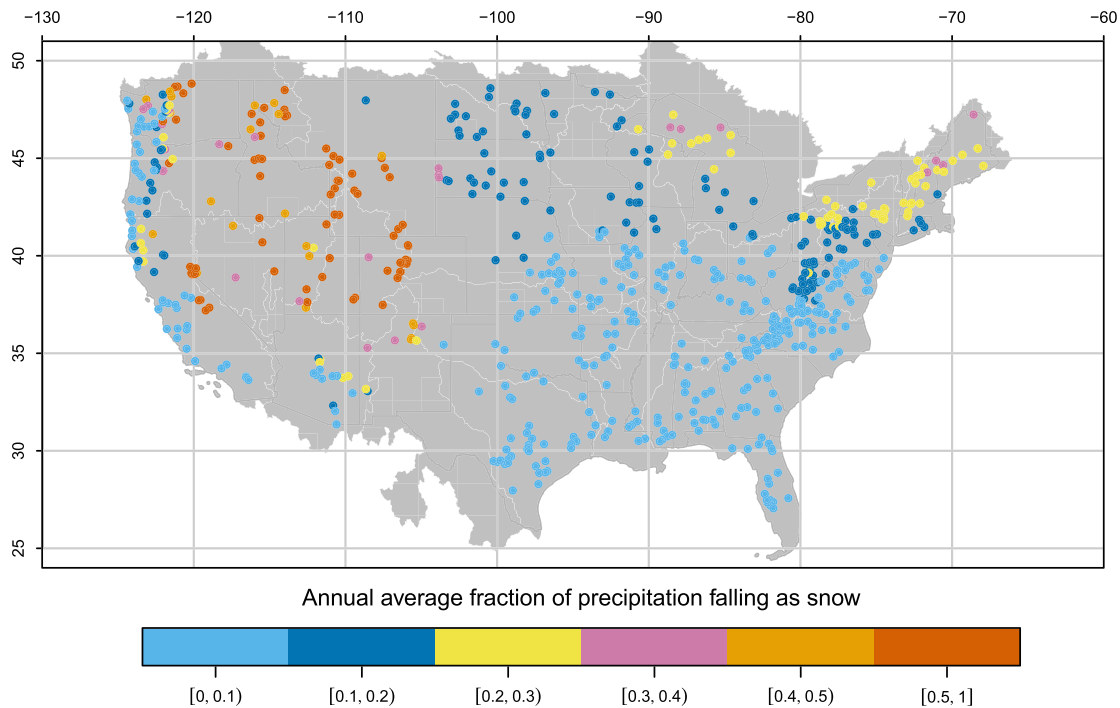


Figure 1. Location of CAMELS catchment outlets across the CONUS. Each catchment was classified into one of the six groups based on the average fraction of annual precipitation falling as snow (f_{snow} ; categories were defined at 0.1 intervals, with all catchments having f_{snow} of at least 0.5 grouped into one category). The 18 major water resources regions over the CONUS are also shown (gray polygons bounded by white lines) for reference (see also Figure S1 in supporting information).

$P_{sm,DOYMAX}$ (for the second), and $P_{eff,MAX}$ and $P_{eff,DOYMAX}$ (for the third). Note that evapotranspiration is only available from October 1980 onward; thus, $P_{eff,MAX}$ and $P_{eff,DOYMAX}$ are not available for 1980.

2.3. Assessing the Correlation Between the Spatial Pattern of Changes in Precipitation Extremes and the Spatial Pattern of Changes in Floods

We calculated temporal changes in the magnitude of AMAX streamflow (Q_{MAX}) and changes in precipitation extreme intensity (P_{MAX} , $P_{sm,MAX}$, and $P_{eff,MAX}$) using normalized Theil-Sen slope (Gudmundsson et al., 2019; Stahl et al., 2012) as follows:

$$\tau_c = \text{median}\left(\frac{x_j - x_i}{j - i}\right) \quad (1)$$

$$T_c = \frac{\tau_c \times 10 \text{years}}{\bar{x}_c} \times 100 \quad (2)$$

where τ_c is the Theil-Sen slope estimator for catchment c , which is defined as the median of the average annual difference in AMAX values (x) between all possible pairs of years. The indices i and j represent year numbers such that $i \in [1, n_c - 1]$, $j \in [2, n_c]$, $i < j$, and n_c is the number of years in the data record (after the screening process described above) for each catchment. T_c is the normalized trend, expressed as a percentage of change per decade relative to the mean of all AMAX values in a catchment (\bar{x}_c). This approach leads to four T_c values for each catchment, one for Q_{MAX} and three for precipitation intensity (P_{MAX} , $P_{sm,MAX}$, and $P_{eff,MAX}$).

To evaluate whether the spatial pattern of changes in floods can be explained by the spatial pattern of changes in precipitation extremes, we calculated the coefficient of determination R^2 (Rao, 1973), which is the square of the correlation between the T_c values of Q_{MAX} and the T_c values of a precipitation extreme metric (e.g., T_c of P_{MAX}). The value of R^2 ranges from 0 to 1, and a high R^2 indicates a strong correlation.

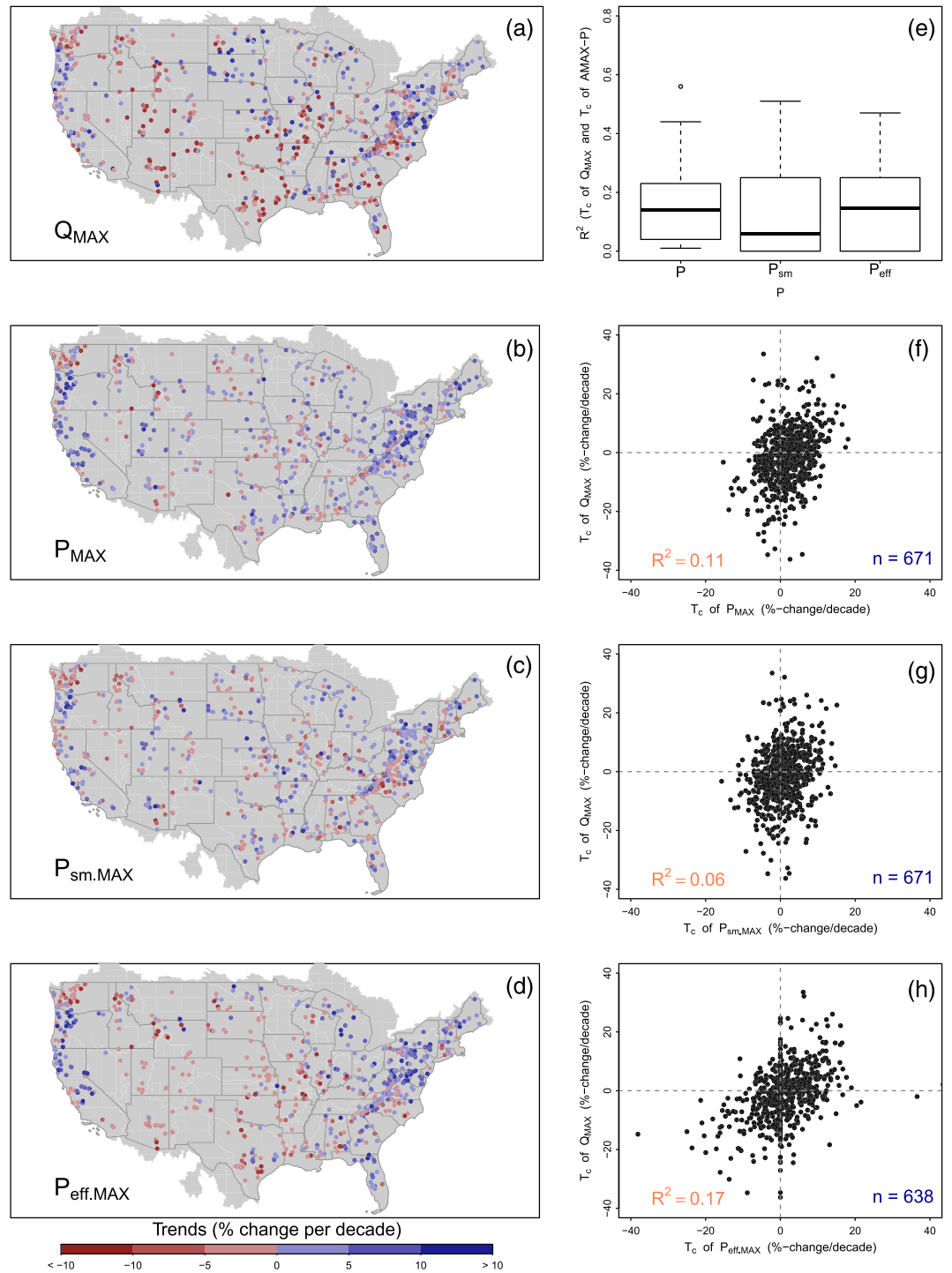


Figure 2. Trends in (a) Q_{MAX} , (b) P_{MAX} , (c) $P_{sm,MAX}$, and (d) $P_{eff,MAX}$ across each of the 671 CAMELS catchments based on the normalized Thiel-Sen slope (T_c). Scatter plots between T_c values of Q_{MAX} and T_c values of (f) P_{MAX} , (g) $P_{sm,MAX}$, and (h) $P_{eff,MAX}$ are also shown. (e) Boxplot of the R^2 between T_c values of annual floods and T_c values of annual precipitation extremes (see Figure S2 in the supporting information for disaggregation of results across water resources regions).

2.4. Assessing the Linkage Between Precipitation Extremes and Floods

To quantify the strength of a potential relationship between precipitation extremes and floods, we took the probability approach (Ivancic & Shaw, 2015; Ledingham et al., 2019) and identified the annual precipitation extremes that were followed closely (in time) by an annual flood extreme in each catchment. Specifically, we matched the timing of AMAX precipitation events (represented by P_{DOYMAX} , $P_{sm.DOYMAX}$, and $P_{eff.DOYMAX}$ indices) and the timing of annual floods (represented by Q_{DOYMAX} index; see supporting information Figures S3–S5 for more details). The co-occurrence probability was then computed as the fraction of annual precipitation extremes that can be directly linked to annual floods. To account for travel time required for precipitation to reach a catchment outlet, we adopted a previous approach (Ivancic & Shaw, 2015) and allowed a lag of up to 5 days (i.e., we presume a connection if $0 \leq Q_{DOYMAX} - P_{DOYMAX} \leq 5$). This lag is well suited our objective—to investigate the linkages between precipitation extremes and annual floods—as the chosen catchments have a relatively small size and thus a time of concentration of less than 5 days (Pilgrim et al., 1987). If precipitation extremes and floods were independent, the probability of a match, on average, would be less than 2%, which is the random chance of Q_{DOYMAX} having a value between P_{DOYMAX} and $P_{DOYMAX} + 5$ (6 days) of all possible days in a nonleap year (365 days).

Given the importance of precipitation type (i.e., snow or rain) over much of the CONUS (Berghuijs et al., 2016), as well as other parts of the world (Blöschl et al., 2017; Do, Westra, et al., 2020), we also assessed whether relationships between precipitation extremes and floods vary by precipitation type. We used the annual average proportion of precipitation that falls as snow, readily available in Addor et al. (2017b), and is denoted as f_{snow} . Each catchment was classified into one of the six categories; the first five are defined by f_{snow} values between 0.0 and 0.5 at intervals of 0.1; the sixth category includes all catchments with an f_{snow} value between 0.5 and 1.0 (see Figure 1). We then assessed whether there are significant differences in the co-occurrence probability of precipitation extremes and floods across f_{snow} classification categories.

2.5. Assessing Temporal Correlation Between the Intensity of Precipitation Extremes and Flood Magnitude

We identified catchments with a similar fraction of co-occurrence between precipitation extremes and floods by grouping catchments into seven groups according to the co-occurrence probability at 0.1 intervals (note that all catchments with at least 0.6 co-occurrence probability were grouped into one category). We then measured the covariation between the intensity of precipitation extremes (e.g., P_{MAX} index) and the magnitude of floods (Q_{MAX} index) at each catchment using the coefficient of determination R^2 . The R^2 values were then analyzed alongside the co-occurrence probability to quantify the extent of which changes in precipitation extremes are useful to infer changes in flood magnitude.

3. Results and Discussions

3.1. A Low Correlation Between the Spatial Pattern of Changes in Floods and the Spatial Pattern of Changes in Precipitation Extremes

Figure 2 shows temporal changes in the magnitude of annual floods and precipitation extremes across the CAMELS catchments. We note that the effective precipitation (P_{eff}) could be equal to zero throughout the year wherever precipitation could not make the catchment fully saturated. Specifically, there are 110 catchments having zero $P_{eff.MAX}$ over more than 20 years, leading to a zero Thiel-Sen slope estimated as shown in Figure 2h (see also supporting information Figure S2). We also removed 33 catchments that have $P_{eff.MAX}$ equal to zero across all years from our analyses, leading to a sample size of 638 catchments for $P_{eff.MAX}$ assessment.

Over the reference period, more CAMELS catchments (53%) experienced a decrease in Q_{MAX} index (Figure 2a), consistent with recent investigations (Do et al., 2017; Do, Zhao, et al., 2020; Gudmundsson et al., 2019; Hodgkins et al., 2017, 2019). On the contrary, P_{MAX} index shows an increasing trend (Figure 2b) over the majority of catchments (67%), although some interior water resources regions exhibited a more prominent decreasing trend (e.g., Missouri Region; see Figure S2 in the supporting information for trends in annual floods and precipitation extremes over individual regions). There is a low correlation between the spatial pattern of changes in P_{MAX} and the spatial pattern of changes in Q_{MAX} (Figure 2f) with

an R^2 of 0.11, indicating that only 11% of the spatial variation of trends of Q_{MAX} can be explained using trends of P_{MAX} .

The spatial pattern of $P_{sm,MAX}$ trends (Figure 2c) is generally consistent with that of P_{MAX} trends, while the spatial pattern of $P_{eff,MAX}$ trends (Figure 2d) shows a substantial difference relative to that of P_{MAX} trends and appears to be more consistent with the spatial pattern of Q_{MAX} trends. The coefficient of determination between precipitation extreme trends and Q_{MAX} trends supports this finding, with an R^2 of 0.06 and 0.17 for $P_{sm,MAX}$ trends and $P_{eff,MAX}$ trends, respectively (Figures 2g and 2h). These results are generally expected, as the snow-soil routine underlying $P_{eff,MAX}$ can be seen as a simple conceptual model that takes into account several catchment processes.

More importantly, the R^2 values between Q_{MAX} trends and precipitation extreme trends are less than 0.2 across all precipitation extreme metrics. This result means that the spatial variation of precipitation extreme trends can explain less than 20% of the spatial variation of Q_{MAX} trends across the CONUS from 1980 to 2014. The R^2 is also low over individual water resources regions (Figure 2e), even though some regions have most catchments associated with a fraction of annual precipitation falling as snow of less than 0.1 (e.g., the Texas-Gulf Region and the South Atlantic-Gulf Region). Specifically, more than 60% of the regions have an R^2 value of less than 0.2 (scatter plots for individual regions were provided in Figure S2 of the supporting information), indicating the limitation of using trends of precipitation extremes to infer trends of floods.

3.2. Co-occurrence Probability of Precipitation Extremes and Floods Across the CONUS

The low correlation between the spatial pattern of changes in precipitation extremes and that of floods (discussed in section 3.1) is potentially attributable to a weak linkage between these variables, as there are other mechanisms that could trigger floods (Blöschl et al., 2019; Merz & Blöschl, 2003). To quantify the linkage between these extremes, we assessed the co-occurrence probability between precipitation extremes and floods over individual catchments and the results are shown in Figure 3 (see Figures S3–S5 in the supporting information for Q_{DOYMAX} , P_{DOYMAX} , $P_{sm,DOYMAX}$, and $P_{eff,DOYMAX}$ across all catchments). The averaged co-occurrence probability across all catchments is 32%, 30%, and 37% for P_{DOYMAX} , $P_{sm,DOYMAX}$, and $P_{eff,DOYMAX}$, respectively. This number is consistent with a previous investigation (Ivancic & Shaw, 2015), indicating that annual precipitation extremes can only be linked directly to about one third of the annual flood population.

The vast majority of catchments (more than 95%) have a co-occurrence probability that is much higher than random chance (i.e., 2%), which is generally expected. Catchments with a relatively high co-occurrence probability are mostly located in coastal regions (e.g., South Atlantic-Gulf Region, Texas Gulf Region, California Region, and Pacific Northwest Region), while co-occurrence probability tends to be low whenever the fraction of precipitation falling as snow (f_{snow}) is high (e.g., Upper Colorado Region and Great Basin Region). More importantly, only a small fraction (14%) of all catchments has a co-occurrence probability between Q_{DOYMAX} and P_{DOYMAX} (Figure 3a; see Figure S6 for regional results) of at least 0.5, indicating a weak linkage.

The co-occurrence probability between Q_{DOYMAX} and $P_{sm,DOYMAX}$ (Figure 3b; see Figure S7 for regional results) is higher than or equal to 0.5 over 7% of all catchments, indicating a weaker linkage relative to that between Q_{DOYMAX} and P_{DOYMAX} . A possible reason is that soil moisture has a relatively strong seasonal cycle (Eltahir, 1998; Findell & Eltahir, 1997), contrasting to a weak seasonality of short-duration precipitation extremes (Do, Westra, et al., 2020). Using P_{sm} has potentially excluded many short-duration flood-induced rainfall events that spread throughout the years, including the months with a low soil moisture content. The removal of these flood-induced rainfall events is potentially the reason for a lower co-occurrence probability between Q_{DOYMAX} and $P_{sm,DOYMAX}$ relative to that between Q_{DOYMAX} and P_{DOYMAX} .

Among the three precipitation extreme metrics, effective precipitation (Figure 3c; see Figure S8 for regional results) is the variable with the highest co-occurrence probability to floods. Specifically, 26% of all catchments have a co-occurrence probability between $P_{eff,DOYMAX}$ and Q_{DOYMAX} of at least 0.5. A simple approach to take into account snow-soil interaction has led to a substantial increase in co-occurrence probability, suggesting that catchment processes potentially play a more important role in modulating floods relative to precipitation intensity.

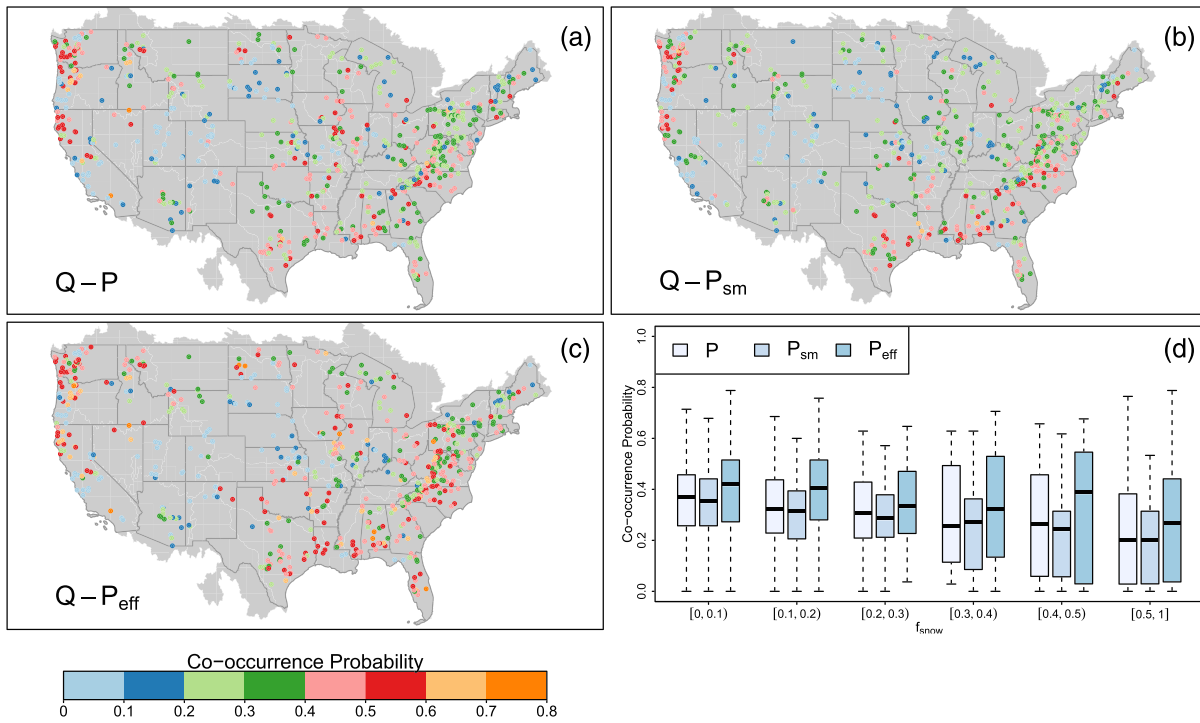


Figure 3. Co-occurrence probability between AMAX streamflow and (a) AMAX precipitation, (b) AMAX wet-month precipitation, (c) AMAX effective precipitation across all CAMELS catchments, and (d) when grouped into six categories using the fraction of precipitation falling as snow (f_{snow}). Note that P_{eff} were available for only 638 catchments.

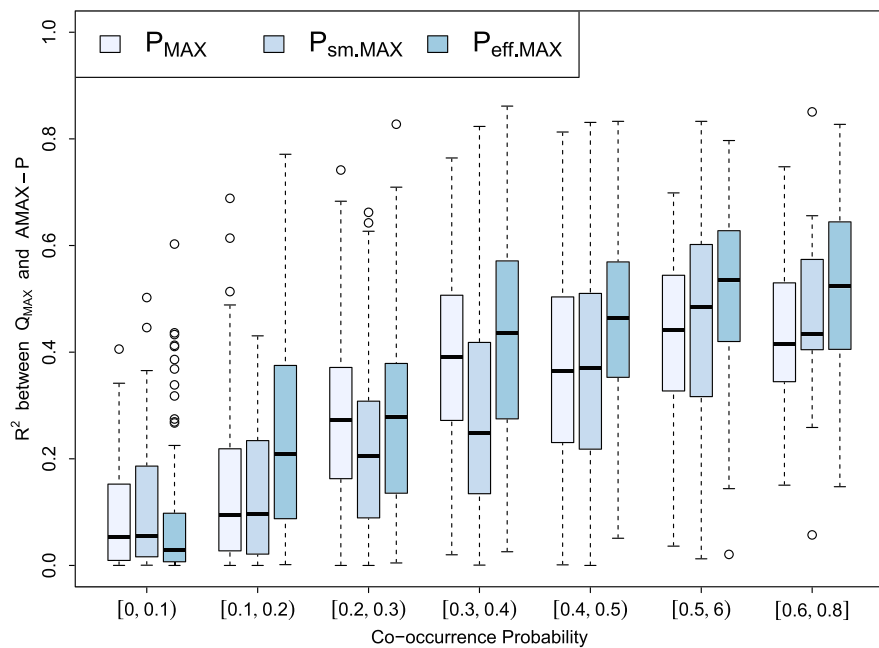


Figure 4. Coefficient of determination (R^2) between AMAX discharges and AMAX precipitation across all CAMELS catchments, grouped by the co-occurrence probability. Results are showed for precipitation (P), wet-month precipitation (P_{sm}), and effective precipitation (P_{eff}). Note that P_{eff} were available for only 638 catchments.

When catchments are divided into different categories using f_{snow} (Figure 3d), there is a notable decrease of co-occurrence probability when f_{snow} increases. We note that the co-occurrence probability between precipitation extremes and floods is not consistently low across all catchments with a high f_{snow} . For instance, of all 73 catchments with an f_{snow} of higher than or equal to 0.5, six catchments (located in the Pacific Northwest Region) have a co-occurrence probability between P_{DOYMAX} and Q_{MAX} of at least 0.5. As a result, catchments with a high snow-to-rain ratio are likely to have floods not driven by precipitation extremes, but there are exceptions such as catchments strongly influenced by atmospheric rivers which are responsible for flood-induced rainfall events.

3.3. To What Extent Are Changes in Precipitation Extremes Useful to Explain Changes in Floods?

The covariation between precipitation extremes and Q_{MAX} is relatively low, with 81%, 85%, and 66% of all catchments having an R^2 of less than 0.5 for P_{MAX} , $P_{sm.MAX}$, and $P_{eff.MAX}$, respectively. When catchments are grouped into different categories according to co-occurrence probability, a strong positive relationship between covariation and co-occurrence probability is observed (Figure 4). Of all catchments with co-occurrence probability of less than 0.5, the averaged R^2 is 0.28 (for P_{MAX}), 0.24 (for $P_{sm.MAX}$), and 0.33 (for $P_{eff.MAX}$), respectively, indicating that only about 30% of the temporal variability of floods can be explained by precipitation extremes.

Focusing on the catchments with the highest co-occurrence probability (at least 0.6), a low-to-moderate correlation is observed, with the median of R^2 between Q_{MAX} and precipitation extremes that is 0.41, 0.43, and 0.52 for P_{MAX} , $P_{sm.MAX}$, and $P_{eff.MAX}$, respectively. The covariation between $P_{eff.MAX}$ and Q_{MAX} is the highest, with 34 out of 63 catchments (54%) have an R^2 of above 0.5. The covariation between P_{MAX} and Q_{MAX} is the lowest, with 10 out of 28 catchments (36%) have an R^2 value of above 0.5, further confirming the need for considering catchment processes (e.g., snow-soil interaction) to explain changes in annual floods.

4. Summary and Conclusions

Using annual maxima precipitation and streamflow across a large sample of catchments, this study has empirically assessed the relationship between temporal changes in precipitation extremes and changes in annual flood magnitude. The spatial pattern of trends detected from precipitation extremes is weakly correlated to the spatial pattern of trends detected from AMAX streamflow over 671 CONUS catchments, with a coefficient of determination of less than 0.2.

A weak linkage between annual precipitation extremes and annual floods is apparent across the CAMELS catchments, with the vast majority of catchments having less than 50% of annual flood events directly linked to precipitation extremes (85%, 90%, and 73% of all catchments for AMAX precipitation, AMAX wet-month precipitation, and AMAX effective precipitation, respectively). Catchments with a high snow-to-rain ratio generally have a low co-occurrence probability between precipitation extremes and floods, but the impact of snow presence is not uniform. The covariation between extreme precipitation intensity and flood magnitude is also low, with more than 60% of catchments having an R^2 of less than 0.5, regardless of which precipitation extreme metrics being used. Using a snow-soil routine to correct the actual amount of precipitation modulating floods has led to a substantially improved predictability for changes in floods, suggesting that future trend detection studies should focus more on the catchment attributes such as soil profile and impervious area.

Notwithstanding the complex processes driving floods, this study has quantitatively assessed the limitation of using changes in precipitation as a proxy for potential changes in floods. The findings indicate that the intensity of precipitation extremes alone is a weak predictor for temporal changes in annual maxima of daily streamflow, even for catchments with a relatively high co-occurrence probability. It is informative to note that this study focused on relatively small, “near-natural” catchments, and thus, the findings may not be representative for larger catchments or catchments influenced heavily by urbanization. This study highlights the need for additional efforts to investigate the nonlinear responses of floods to climate changes using a larger sample of catchments, which would hopefully achieve a universal understanding of how floods might evolve. For instance, the approach presented in this study can be applied for other large sample data sets (Addor et al., 2019; Alvarez-Garreton et al., 2018; Coxon et al., 2020; Gudmundsson et al., 2018) to quantify the contribution of extreme precipitation to historical changes in floods for other parts of the world.

Data Availability Statement

Hydrometeorological data are freely available at <https://dx.doi.org/10.5065/D6MW2F4D> (Newman et al., 2014), while the catchment attributes, including the fraction of precipitation falling as snow, are freely available at <https://doi.org/10.5065/D6G73C3Q> (Addor et al., 2017a).

Acknowledgments

Hong Xuan Do is currently funded by the School for Environment and Sustainability, University of Michigan through Grant U064474. The authors appreciate the developers of the CAMELS data set for making this asset publicly available.

References

- Addor, N., Do, H. X., Alvarez-Garreto, C., Coxon, G., Fowler, K., & Mendoza, P. (2019). Large-sample hydrology: Recent progress, guidelines for new datasets and grand challenges. *Hydrological Sciences Journal*.
- Addor, N., Newman, A. J., Mizukami, N., & Clark, M. P. (2017a). The CAMELS data set: catchment attributes and meteorology for large-sample studies. *version 2.0*. Boulder, CO: UCAR/NCAR. <https://doi.org/10.5065/D6G73C3Q>
- Addor, N., Newman, A. J., Mizukami, N., & Clark, M. P. (2017b). The CAMELS data set: Catchment attributes and meteorology for large-sample studies. *Hydrology and Earth System Sciences Discussions*, 2017, 1–31.
- Alvarez-Garreton, C., Mendoza, P. A., Boisier, J. P., Addor, N., Galleguillos, M., Zambrano-Bigiarini, M., et al. (2018). The CAMELS-CL dataset: Catchment attributes and meteorology for large sample studies—Chile dataset. *Hydrology and Earth System Sciences*, 22(11), 5817–5846. <https://doi.org/10.5194/hess-22-5817-2018>
- Archfield, S. A., Hirsch, R. M., Viglione, A., & Blöschl, G. (2016). Fragmented patterns of flood change across the United States. *Geophysical Research Letters*, 43, 10,232–10,239. <https://doi.org/10.1002/2016GL070590>
- Berghuijs, W. R., Harrigan, S., Molnar, P., Slater, L. J., & Kirchner, J. W. (2019). The relative importance of different flood-generating mechanisms across Europe. *Water Resources Research*, 55, 4582–4593. <https://doi.org/10.1029/2019WR024841>
- Berghuijs, W. R., Woods, R. A., Hutton, C. J., & Sivapalan, M. (2016). Dominant flood generating mechanisms across the United States. *Geophysical Research Letters*, 43, 4382–4390. <https://doi.org/10.1002/2016GL068070>
- Blöschl, G., Hall, J., Parajka, J., Perdigão, R. A. P., Merz, B., Arheimer, B., et al. (2017). Changing climate shifts timing of European floods. *Science*, 357(6351), 588–590. <https://doi.org/10.1126/science.aan2506>
- Blöschl, G., Hall, J., Viglione, A., Perdigão, R. A., Parajka, J., Merz, B., et al. (2019). Changing climate both increases and decreases European river floods. *Nature*, 573(7772), 108–111. <https://doi.org/10.1038/s41586-019-1495-6>
- Bosilovich, M. G., Schubert, S. D., & Walker, G. K. (2005). Global changes of the water cycle intensity. *Journal of Climate*, 18(10), 1591–1608. <https://doi.org/10.1175/JCLI3357.1>
- Burnash, R. J. C., Ferral, R. L., & McGuire, R. A. (1973). A generalized streamflow simulation system: Conceptual modeling for digital computers, US Department of Commerce, National Weather Service, and State of California.
- Clausius, R. (1850). Über die bewegende Kraft der Wärme und die Gesetze, welche sich daraus für die Wärmelehre selbst ableiten lassen. *Annalen der Physik*, 155(3), 368–397. <https://doi.org/10.1002/andp.18501550306>
- Coxon, G., Addor, N., Bloomfield, J. P., Freer, J., Fry, M., Hannaford, J., et al. (2020). CAMELS-GB: Hydrometeorological time series and landscape attributes for 671 catchments in Great Britain. *Earth System Science Data Discussions*, 2020, 1–34.
- Do, H. X., Gudmundsson, L., Leonard, M., & Westra, S. (2018). The global streamflow indices and metadata archive (GSIM)—Part 1: The production of a daily streamflow archive and metadata. *Earth System Science Data*, 10(2), 765–785. <https://doi.org/10.5194/essd-10-765-2018>
- Do, H. X., Westra, S., Leonard, M., & Gudmundsson, L. (2020). Global-scale prediction of flood timing using atmospheric reanalysis. *Water Resources Research*, 56, e2019WR024945. <https://doi.org/10.1029/2019WR024945>
- Do, H. X., Westra, S., & Michael, L. (2017). A global-scale investigation of trends in annual maximum streamflow. *Journal of Hydrology*, 552, 28–43. <https://doi.org/10.1016/j.jhydrol.2017.06.015>
- Do, H. X., Zhao, F., Westra, S., Leonard, M., Gudmundsson, L., Boulange, J. E. S., et al. (2020). Historical and future changes in global flood magnitude—Evidence from a model–observation investigation. *Hydrology and Earth System Sciences*, 24(3), 1543–1564. <https://doi.org/10.5194/hess-24-1543-2020>
- Donat, M. G., Alexander, L. V., Yang, H., Durre, I., Vose, R., Dunn, R. J. H., et al. (2013). Updated analyses of temperature and precipitation extreme indices since the beginning of the twentieth century: The HadEX2 dataset. *Journal of Geophysical Research: Atmospheres*, 118, 2098–2118. <https://doi.org/10.1002/jgrd.50150>
- Eltahir, E. A. B. (1998). A soil moisture–rainfall feedback mechanism: 1. Theory and observations. *Water Resources Research*, 34(4), 765–776. <https://doi.org/10.1029/97WR03499>
- Findell, K. L., & Eltahir, E. A. B. (1997). An analysis of the soil moisture–rainfall feedback, based on direct observations from Illinois. *Water Resources Research*, 33(4), 725–735. <https://doi.org/10.1029/96WR03756>
- Gronewold, A. D., & Stow, C. A. (2014). Water loss from the Great Lakes. *Science*, 343(6175), 1084–1085. <https://doi.org/10.1126/science.1249978>
- Gudmundsson, L., Do, H. X., Leonard, M., & Westra, S. (2018). The global streamflow indices and metadata archive (GSIM)—Part 2: Time series indices and homogeneity assessment, edited, PANGAEA.
- Gudmundsson, L., Leonard, M., Do, H. X., Westra, S., & Seneviratne, S. I. (2019). Observed trends in global indicators of mean and extreme streamflow. *Geophysical Research Letters*, 46, 756–766. <https://doi.org/10.1029/2018GL079725>
- Guerreiro, S. B., Fowler, H. J., Barbero, R., Westra, S., Lenderink, G., Blenkinsop, S., et al. (2018). Detection of continental-scale intensification of hourly rainfall extremes. *Nature Climate Change*, 8(9), 803–807. <https://doi.org/10.1038/s41558-018-0245-3>
- Hock, R. (2003). Temperature index melt modelling in mountain areas. *Journal of Hydrology*, 282(1–4), 104–115. [https://doi.org/10.1016/S0022-1694\(03\)00257-9](https://doi.org/10.1016/S0022-1694(03)00257-9)
- Hodgkins, G. A., Dudley, R. W., Archfield, S. A., & Renard, B. (2019). Effects of climate, regulation, and urbanization on historical flood trends in the United States. *Journal of Hydrology*, 573, 697–709. <https://doi.org/10.1016/j.jhydrol.2019.03.102>
- Hodgkins, G. A., Whitfield, P. H., Burn, D. H., Hannaford, J., Renard, B., Stahl, K., et al. (2017). Climate-driven variability in the occurrence of major floods across North America and Europe. *Journal of Hydrology*, 552, 704–717. <https://doi.org/10.1016/j.jhydrol.2017.07.027>
- Huntington, T. G. (2006). Evidence for intensification of the global water cycle: Review and synthesis. *Journal of Hydrology*, 319(1–4), 83–95. <https://doi.org/10.1016/j.jhydrol.2005.07.003>
- Ivancic, T., & Shaw, S. (2015). Examining why trends in very heavy precipitation should not be mistaken for trends in very high river discharge. *Climatic Change*, 1–13.

- Keenan, R. J., Reams, G. A., Achard, F., de Freitas, J. V., Grainger, A., & Lindquist, E. (2015). Dynamics of global forest area: Results from the FAO Global Forest Resources Assessment 2015. *Forest Ecology and Management*, 352, 9–20. <https://doi.org/10.1016/j.foreco.2015.06.014>
- Kundzewicz, Z. W., Graczyk, D., Maurer, T., Przymusińska, I., Radziejewski, M., Svensson, C., & Szwed, M. (2004). *Detection of change in world-wide hydrological time series of maximum annual flow*. Koblenz, Germany: Global Runoff Date Centre.
- Lambin, E. F., Geist, H. J., & Lepers, E. (2003). Dynamics of land-use and land-cover change in tropical regions. *Annual Review of Environment and Resources*, 28(1), 205–241. <https://doi.org/10.1146/annurev.energy.28.050302.105459>
- Ledingham, J., Archer, D., Lewis, E., Fowler, H., & Kilsby, C. (2019). Contrasting seasonality of storm rainfall and flood runoff in the UK and some implications for rainfall-runoff methods of flood estimation. *Hydrology Research*, 50(5), 1309–1323. <https://doi.org/10.2166/nh.2019.040>
- Lins, H. F., & Slack, J. R. (1999). Streamflow trends in the United States. *Geophysical Research Letters*, 26(2), 227–230. <https://doi.org/10.1029/1998GL900291>
- Merz, R., & Blöschl, G. (2003). A process typology of regional floods. *Water Resources Research*, 39(12), 1340. <https://doi.org/10.1029/2002WR001952>
- Milly, P. C. D., Betancourt, J., Falkenmark, M., Hirsch, R. M., Kundzewicz, Z. W., Lettenmaier, D. P., & Stouffer, R. J. (2008). Stationarity is dead: Whither water management? *Science*, 319(5863), 573–574. <https://doi.org/10.1126/science.1151915>
- Newman, A. J., Clark, M. P., Sampson, K., Wood, A., Hay, L. E., Bock, A., et al. (2015). Development of a large-sample watershed-scale hydrometeorological data set for the contiguous USA: Data set characteristics and assessment of regional variability in hydrologic model performance. *Hydrology and Earth System Sciences*, 19(1), 209–223. <https://doi.org/10.5194/hess-19-209-2015>
- Newman, A. J., Sampson, K., Clark, M. P., Bock, A., Viger, R. J., & Blodgett, D. (2014). A large-sample watershed-scale hydrometeorological dataset for the contiguous USA, *UCAR/NCAR, doi*, 10, D6MW2F4D.
- Papalexiou, S. M., & Montanari, A. (2019). Global and regional increase of precipitation extremes under global warming. *Water Resources Research*, 55, 4901–4914. <https://doi.org/10.1029/2018WR024067>
- Pilgrim, E., A. Institution of Engineers, Pilgrim, D., & Canterford, R. (1987). *Australian rainfall and runoff*. Australia: Institution of Engineers.
- Rao, C. R. (1973). *Linear statistical inference and its applications* (p. 625). New York: Wiley.
- Sharma, A., Wasko, C., & Lettenmaier, D. P. (2018). If precipitation extremes are increasing, why aren't floods? *Water Resources Research*, 54, 8545–8551. <https://doi.org/10.1029/2018WR023749>
- Slater, L. J., Singer, M. B., & Kirchner, J. W. (2015). Hydrologic versus geomorphic drivers of trends in flood hazard. *Geophysical Research Letters*, 42, 370–376. <https://doi.org/10.1002/2014GL062482>
- Stahl, K., Tallaksen, L. M., Hannaford, J., & van Lanen, H. A. J. (2012). Filling the white space on maps of European runoff trends: Estimates from a multi-model ensemble. *Hydrology and Earth System Sciences*, 16(7), 2035–2047. <https://doi.org/10.5194/hess-16-2035-2012>
- Stein, L., Pianosi, F., & Woods, R. (2020). Event-based classification for global study of river flood generating processes. *Hydrological Processes*, 34(7), 1514–1529. <https://doi.org/10.1002/hyp.13678>
- Thornton, P. E., Running, S. W., & White, M. A. (1997). Generating surfaces of daily meteorological variables over large regions of complex terrain. *Journal of Hydrology*, 190(3-4), 214–251. [https://doi.org/10.1016/S0022-1694\(96\)03128-9](https://doi.org/10.1016/S0022-1694(96)03128-9)
- Van den Dool, H., Huang, J., & Fan, Y. (2003). Performance and analysis of the constructed analogue method applied to US soil moisture over 1981–2001. *Journal of Geophysical Research*, 108(D16), 8617. <https://doi.org/10.1029/2002JD003114>
- Villarini, G., & Smith, J. A. (2010). Flood peak distributions for the eastern United States. *Water Resources Research*, 46, W06504. <https://doi.org/10.1029/2009WR008395>
- Wasko, C., Nathan, R., & Peel, M. C. (2020). Changes in antecedent soil moisture modulate flood seasonality in a changing climate. *Water Resources Research*, 56, e2019WR026300. <https://doi.org/10.1029/2019WR026300>
- Westra, S., Alexander, L. A., & Zwiers, F. W. (2013). Global increasing trends in annual maximum daily precipitation. *Journal of Climate*, 26(11), 15.
- Westra, S., Fowler, H. J., Evans, J. P., Alexander, L. V., Berg, P., Johnson, F., et al. (2014). Future changes to the intensity and frequency of short-duration extreme rainfall. *Reviews of Geophysics*, 52, 522–555. <https://doi.org/10.1002/2014RG000464>
- Woods, R. A. (2009). Analytical model of seasonal climate impacts on snow hydrology: Continuous snowpacks. *Advances in Water Resources*, 32(10), 1465–1481. <https://doi.org/10.1016/j.advwatres.2009.06.011>
- Yamazaki, D., O'Loughlin, F., Trigg, M. A., Miller, Z. F., Pavelsky, T. M., & Bates, P. D. (2014). Development of the global width database for large rivers. *Water Resources Research*, 50, 3467–3480. <https://doi.org/10.1002/2013WR014664>
- Ye, S., Li, H.-Y., Leung, L. R., Guo, J., Ran, Q., Demissie, Y., & Sivapalan, M. (2017). Understanding flood seasonality and its temporal shifts within the contiguous United States. *Journal of Hydrometeorology*, 18(7), 1997–2009. <https://doi.org/10.1175/JHM-D-16-0207.1>